IONIC CHANNELS WITH CONFORMATIONAL SUBSTATES

P. LÄUGER
Department of Biology, University of Konstanz, D - 7750 Konstanz, Federal Republic of Germany

ABSTRACT Recent studies of protein dynamics suggest that ionic channels can assume many conformational substates. Long-lived substates have been directly observed in single-channel current records. In many cases, however, the lifetimes of conformational states will be far below the theoretical limit of time resolution of single-channel experiments. The existence of such hidden substates may strongly influence the observable (time-averaged) properties of a channel, such as the concentration dependence of conductance. A channel exhibiting fast, voltage-dependent transitions between different conductance states may behave as an intrinsic rectifier. In the presence of more than one permeable ion species, coupling between ionic fluxes may occur, even when the channel has only a single ion-binding site. In special situations the rate of ion translocation becomes limited by the rate of conformational transitions, meaning that the channel approaches the kinetic behavior of a carrier. As a result of the strong coulombic interaction between an ion in a binding site and polar groups of the protein, rate constants of conformational transitions may depend on the occupancy of the binding site. Under this condition a nonequilibrium distribution of conformational states is created when ions are driven through the channel by an external force. This may lead to an apparent violation of microscopic reversibility, i.e., to a situation in which the frequency of transitions from state A to state B is no longer equal to the transition frequency from state B to state A.

INTRODUCTION

Ion movement through a transmembrane protein channel may be described as a series of thermally activated jumps over energy barriers. The potential wells and barriers along the transport pathway are determined by the structure of the protein, i.e., by the spatial distribution of ligands such as oxygen atoms of carbonyl groups. In the traditional treatment of ion transport in channels the energy profile is considered to be fixed, i.e., independent of time and independent of the movement of the ion. Such a description corresponds to an essentially static picture of protein structure. During the last years evidence has been accumulated, however, that proteins can assume many conformational substates and at physiological temperatures rapidly move from one substate to the other (Frauenfelder et al., 1979; Karplus and McCammon, 1983). Support for the dynamic nature of protein structure comes from x-ray diffraction and Mössbauer studies (Huber et al., 1976; Parak et al., 1981), fluorescence depolarization experiments (Lakowicz et al., 1983) and nuclear magnetic resonance (NMR) measurements (Wagner, 1983). These and other studies have shown that internal motions in proteins occur in a wide time range, from picoseconds to seconds.

Direct evidence that ionic channels may assume different conformational states comes from single-channel records obtained by the patch-clamp technique (Sakmann and Neher, 1983). Intermediate conductance levels between the fully open and the fully closed state have been observed, for instance, with acetylcholine-activated end-plate channels (Hamill and Sakmann, 1981; Trautmann, 1982; Auerbach and Sachs, 1983) and with glycine-activated channels in neurons (Hamill et al., 1983). In these systems the lifetimes of the substates were sufficiently long so that transitions could be observed directly in the current records. The detection of fast transitions between substates is limited, however, by the finite bandwidth of the measurement. This means that in many cases the observed single-channel current represents merely an average over unresolved conductance states. As will be discussed below, the existence of such hidden substates may strongly influence the observable properties of the channel, such as the current-voltage characteristic or the concentration dependence of conductance.

Of particular interest is the possibility that ion translocation in the channel becomes coupled to conformational transitions (Frehland, 1979; Läuger et al., 1980). In this case the conductance of the channel explicitly depends on the rate constants of conformational transitions. Such coupling may occur when the average lifetimes of conformational states are of the same order or lower than the dwelling times of ions in the binding sites. The channel may then exhibit unusual flux-coupling behavior in experiments with more than one permeable ion species.

As a result of the strong coulombic interaction between an ion in a binding site and polar groups of the protein, transition rate constants may depend on the occupancy of the binding site. Under this condition a nonequilibrium distribution of conformational states is created when ions are driven through the channel by an external force (a

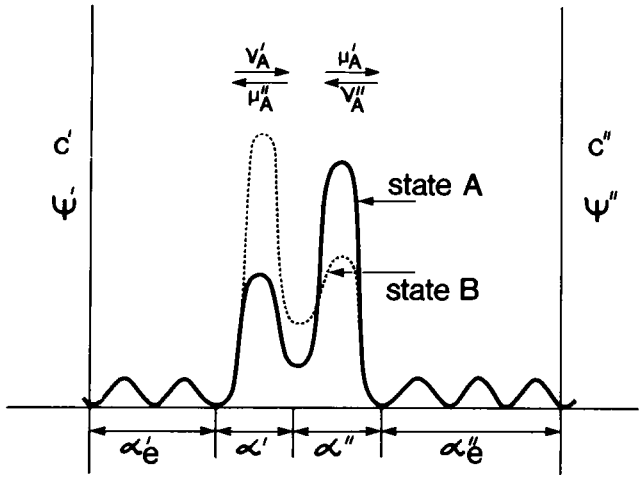

FIGURE 1 Energy profile of a channel with two conformational states A and B. ν'_A and ν''_A are the frequencies of jumps from the solutions into the empty site (state A); μ'_A and μ''_A are the frequencies of jumps from the occupied site into the solutions; c' and c'', and ψ' and ψ'', are the ion concentrations and the electrical potentials in the left and right aqueous solutions. α'_e, α''_e, α', and α'' are dimensionless coefficients describing the fractions of total voltage dropping between solution '' and the respective energy wells. In general, positions of barriers and wells may shift during a conformational transition.

difference of electrochemical potential). As will be shown below, this may lead to an apparent violation of microscopic reversibility, i.e., to a situation in which the frequency of transitions from state A to state B is no longer equal to the transition frequency from state B to state A.

TWO-STATE CHANNEL WITH SINGLE BINDING SITE

We consider a channel that fluctuates between two conducting states A and B, and assume that the rate of ion flow through the channel is limited by two (main) barriers on either side of a single (main) binding site (Fig. 1). In series with the rate-limiting barriers, smaller barriers may be present along the pathway of the ion. This model corresponds to a channel consisting of a wide, water-filled pore and a narrow part acting as a selectivity filter (Hille, 1971). Depending on the occupancy of the binding site, the channel may exist in four substates (Fig. 2): A°: conformation A, empty; A*: conformation A, occupied; B°: conformation B, empty; B*: conformation B, occupied. Since an ion in the binding site interacts electrostatically with neighboring polar groups of the protein, the rate constants for transitions between A and B depend, in general, on whether the binding site is empty or occupied (i.e., $k^\circ_{AB} \neq k^*_{AB}$, and $k^\circ_{BA} \neq k^*_{BA}$).

Transitions between empty and occupied states occur by exchange of an ion between the binding site and the left or right aqueous phase (Fig. 1):

$$\nu_A = \nu'_A + \nu''_A = c'\rho'_A + c''\rho''_A \tag{1}$$

$$\mu_A = \mu'_A + \mu''_A. \tag{2}$$

Similar equations hold for state B. In Eq. 1 it is assumed that ions in the energy wells outside the rate-limiting barriers are always in equilibrium with the corresponding aqueous phase. The jumping frequencies ν'_A and ν''_A into the empty site are then proportional to the aqueous ion concentrations c' and c'', respectively, whereas the rate constants μ'_A and μ''_A for leaving the site are independent of c' and c''.

The principle of microscopic reversibility requires that the rate constants obey the following relationship (Läuger et al., 1980):

$$\frac{\nu'_A\mu'_A}{\nu''_A\mu''_A} = \frac{\nu'_B\mu'_B}{\nu''_B\mu''_B} = \frac{\nu'_A\mu'_B}{\nu''_B\mu''_A} \cdot \frac{k^*_{AB}k^\circ_{BA}}{k^\circ_{AB}k^*_{BA}} = \exp[z(u - u_o)], \tag{3}$$

where z is the valence of the permeable ion species, u the voltage across the channel, and u_o the equilibrium voltage of the ion, both expressed in units of kT/e_o (k, Boltzmann's constant; T, absolute temperature; e_o, elementary charge):

$$u = \frac{\psi' - \psi''}{kT/e_o} \tag{4}$$

$$zu_o = \ln(c''/c'). \tag{5}$$

If $P(X)$ is the probability that a given channel molecule is in state X, the time-averaged single-channel ion flux Φ from solution ' to solution '' (Fig. 1) is given by

$$\Phi = \nu'_A P(A^\circ) - \mu''_A P(A^*) + \nu'_B P(B^\circ) - \mu''_B P(B^*). \tag{6}$$

The probabilities $P(X)$ may be obtained from the steady-state conditions $dP(X)/dt = 0$, introducing the equilibrium constants H° and H^* of the conformational transitions (Läuger et al., 1980):

$$H^\circ = k^\circ_{AB}/k^\circ_{BA}; \qquad H^* = k^*_{AB}/k^*_{BA}. \tag{7}$$

The result reads:

$$\begin{aligned}\Phi = {} & (1/\sigma)[1 - \exp(zu_o - zu)] \\ & \cdot [\nu'_A\mu'_A(1 + \nu_B/k^\circ_{BA} + \mu_B/k^*_{BA}) \\ & + \nu'_B\mu'_B(H^\circ H^* + H^*\nu_A/k^\circ_{BA} + H^\circ\mu_A/k^*_{BA}) \\ & + H^*\nu'_A\mu'_B + H^\circ\nu'_B\mu'_A];\end{aligned} \tag{8}$$

$$\begin{aligned}\sigma \equiv {} & (1 + H^\circ)(\mu_A + H^*\mu_B + \mu_A\mu_B/k^*_{BA}) \\ & + (1 + H^*)(\nu_A + H^\circ\nu_B + \nu_A\nu_B/k^\circ_{BA}) \\ & + \nu_A\mu_B(H^*/k^\circ_{BA} + 1/k^*_{BA}) \\ & + \nu_B\mu_A(H^\circ/k^*_{BA} + 1/k^\circ_{BA}).\end{aligned} \tag{9}$$

It is seen from Eqs. 8 and 9 that the ion flux Φ explicitly depends on the rate constants k°_{AB}, k°_{BA}, k^*_{AB}, and k^*_{BA}. This is an expression of the phenomenon of coupling between ion translocation and conformational transitions. Similarly, the steady-state probabilities $P(X)$ not only contain the equilibrium constants H°, H^*, ν_A/μ_A, and ν_B/μ_B but

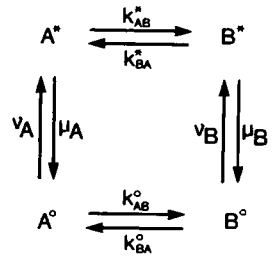

FIGURE 2 Transitions among four substates of a channel with one binding site (A°: conformation A, empty; A*: conformation A, occupied; B°: conformation B, empty; B*: conformation B, occupied).

depend explicitly on the translocation rate constants μ'_A, μ''_A, μ'_B, and μ''_B.

An essential condition for the occurrence of coupling is the assumption that transitions between the two conformations can take place both in the empty and in the occupied state of the binding site. If transitions start only from one of the states (k°_{AB}, $k^\circ_{BA} = 0$ or k^*_{AB}, $k^*_{BA} = 0$), then the dependence of Φ on the rate constants of conformational transitions is lost.

TIME-AVERAGED SINGLE-CHANNEL CONDUCTANCE

If the rate constants of conformational transitions are sufficiently small, many ions pass through the channel during the lifetime of the individual conformational state. In this case a well-defined conductance can be assigned to each state. On the other hand, the frequency of transitions between states A and B may be much too high to be resolved in a single-channel record at the finite bandwidth of the experiment. Apart from instrumental limitations, an inherent restriction is given by thermal fluctuations of the single channel current. According to Nyquist's theorem, the *RMS* value of current noise from a channel of average conductance Λ is $i = \sqrt{4\,kT\Lambda\Delta f}$ in the frequency interval Δf. To observe a transition to a substate, the conductance increment $\Delta\Lambda$ of the substate must be larger than i/V, if V is the driving force of ion flow expressed as a voltage. On the other hand, the detection of a substate of mean lifetime τ requires a bandwidth of $\Delta f > 1/2\pi\tau$. This sets a lower limit of

$$\tau \gtrsim \frac{2kT\Lambda}{\pi(V\Delta\Lambda)^2} \qquad (10)$$

for the lifetime of a substate that can be detected in a single-channel record. With $\Lambda = 10$ pS, $\Delta\Lambda = 1$ pS and $V = 100$ mV, the theoretical limit of τ is of the order of 10 μs. In practice, the resolution may be much lower. Conformational transitions with frequencies not too much above the cutoff frequency of the amplifier manifest themselves as an increased noise of the current signal. If the transitions are still faster, only an average channel current is observed (Fig. 3).

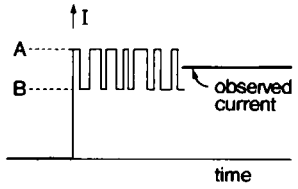

FIGURE 3 If the mean lifetime of conformations A and B are much longer than the dwell times of ions in the binding sites, the channel fluctuates between discrete conductance states. The frequency of transitions between A and B may be much higher than the bandwidth of the measurement; in this case only an average current is observed.

Concentration Dependence of Conductance

Introducing the condition $k^\circ_{AB}, k^*_{AB}, k^\circ_{BA}, k^*_{BA} \ll \nu_A, \nu_B, \mu_A, \mu_B$ (frequency of conformational transitions much smaller than frequency of ion jumps) the ohmic single-channel conductance $\Lambda(c)$ is obtained from Eq. 8 in the form

$$\Lambda(c) = P_A\Lambda_A + (1 - P_A)\Lambda_B \qquad (c' = c'' = c). \qquad (11)$$

$P_A = P(A^\circ) + P(A^*)$ is the probability of finding the channel in state A (A° or A*) which, in the vicinity of equilibrium, is given by

$$P_A = \frac{1 + cK_A}{1 + H^\circ + (1 + H^*)cK_A}. \qquad (12)$$

$K_A = \rho_A/\mu_A$ and $K_B = \rho_B/\mu_B$ are the equilibrium constants of ion binding in states A and B, which are connected by the relation $H^*K_A = H^\circ K_B$ · Λ_A is the conductance of the channel in state A (z is the valency of the ion):

$$\Lambda_A = \frac{z^2e_o^2}{kT} \cdot \frac{cK_A}{1 + cK_A} \cdot \frac{\mu'_A\mu''_A}{\mu_A}. \qquad (13)$$

A similar equation holds for Λ_B. Since P_A is a function of ion concentraton c, the concentration dependence of the observed average conductance Λ is different from the simple saturation characteristic of a channel with time-independent potential profile (Eq. 13).

Deviations from a simple saturation behavior of conductance may result from ion-ion interactions in the channel (Hille and Schwarz, 1978; Urban et al.; 1980; Sandblom et al., 1983) or from the presence of regulatory binding sites. In the channel mechanism discussed here, the single-channel conductance Λ is influenced by the concentration-dependent distribution of conformational states (Eq. 12). The concentration dependence of the probability P_A results from the fact that the equilibrium constants H° and H^* of conformational transitions in the empty and the occupied state of the binding site are, in general, different. Only in the limiting case $H^\circ \approx H^*$ does P_A assume a concentration-independent value $1/(1 + H^\circ)$.

Current-Voltage Characteristic

It has recently been observed that certain ionic channels exhibit a strongly rectifying behavior of single-channel

current amplitudes. Examples are the so-called inwardly rectifying potassium channel that occurs in nerve and muscle cells (Sakmann and Trube, 1984), and the muscarinic potassium channel in pacemaker cells of the mammalian heart (Sakmann et al., 1983). A possible explanation for the asymmetry of the current-voltage characteristic consists in the assumption that the channel fluctuates between different conductance states A and B and that the distribution of the states is voltage dependent (Gunning, 1983). If the transition frequencies are too high to be resolved in a single-channel record, the channel may behave as an intrinsic rectifier.

For a more quantitative discussion we assume that state B is virtually nonconducting ($\mu_B, \nu_B \approx 0$). According to Eq. 8 the channel current $I = ze_0\Phi$ is then given by

$$I = ze_0\nu'_A\mu'_A \frac{1 - \exp[-z(u - u_0)]}{(1 + H^0)\mu_A + (1 + H^*)\nu_A}. \quad (14)$$

If $\alpha' u$ and $\alpha'' u$ are the voltages across the left and right barrier of the selectivity filter (Fig. 1), the voltage dependence of the rate constants μ'_A and μ''_A is given by the following rate-theory expressions (Parlin and Eyring, 1954), assuming symmetrical barriers:

$$\mu'_A = \tilde{\mu}'_A \exp(z\alpha'' u/2); \qquad \mu''_A = \tilde{\mu}''_A \exp(-z\alpha' u/2). \quad (15)$$

$\tilde{\mu}'_A$ and $\tilde{\mu}''_A$ are the values of μ'_A and μ''_A at $u = 0$. Similarly, since the outer parts of the channel are assumed to be in equilibrium with the external solutions:

$$\nu'_A = \rho'_A c' = \tilde{\rho}'_A c' \exp[zu(\alpha'_e + \alpha'/2)] \quad (16)$$

$$\nu''_A = \rho''_A c'' = \tilde{\rho}''_A c'' \exp[-zu(\alpha''_e + \alpha''/2)] \quad (17)$$

$$\alpha'_e + \alpha' + \alpha'' + \alpha''_e = 1. \quad (18)$$

Replacing α'_e, α''_e, α', α'' by β'_e, β''_e, β', β'', analogous expressions for the rate constants in state B are obtained.

To describe the voltage dependence of the equilibrium constants $K^0 = k^0_{AB}/k^0_{BA}$ and $K^* = k^*_{AB}/k^*_{BA}$, we consider the channel molecule as an assembly of point charges q_i (Fig. 4). The q_i may represent free charges as well as charges from dipolar groups. During a transition from state A° to B° the charge $q_i \equiv e_0\theta_i$ is displaced over a certain distance Δl_i. If Δx_i is the component of Δl_i in the direction of the external field E, the contribution of membrane voltage $V = \psi' - \psi''$ to the total energy change during the conformational transition is given by

$$\Delta U = -E\sum_i q_i\Delta x_i = -Ve_0\sum_i \theta_i\Delta x_i/d \equiv -Ve_0\eta^0. \quad (19)$$

The second part of this relation is based on the assumption that the electric field is constant within the membrane. In an analogous way the voltage dependence of the transitions A* → B* is described. This yields

$$H^0 = \tilde{H}^0 \exp(\eta^0 u); \qquad H^* = \tilde{H}^* \exp(\eta^* u). \quad (20)$$

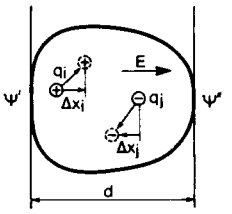

FIGURE 4 The voltage dependence of the equilibrium constants K^0 and K^* of conformational transitions is treated by considering the channel molecule as an assembly of point charges q_i. During a transition from state A° to state B°, the charge q_i is displaced over a certain distance Δx_i in the direction of the external field E. d is the membrane thickness.

$\tilde{H}^0$ and $\tilde{H}^*$ are the values of H^0 and H^* at zero voltage. It is seen from Eqs. 3, 15–18, and 20 that the "gating charges" $e_0\eta^0$ and $e_0\eta^*$ are connected by

$$\eta^* - \eta^0 = z[\beta'_e + \beta' - (\alpha'_e + \alpha')]. \quad (21)$$

The quantity $\beta'_e + \beta' - (\alpha'_e + \alpha')$ describes the displacement of the binding site within the membrane dielectric during the conformational transition A → B.

Current-voltage curves (Eq. 14) of a channel that fluctuates between a conducting state A and a nonconducting state B are shown in Fig. 5 for symmetrical aqueous solutions ($c' = c''$) and different values of the equilibrium constants $\tilde{H}^0 = \tilde{H}^* \equiv \tilde{H}$. The same gating charge of $+2e_0$ has been assumed for both transitions A° → B° and A* → B* ($\eta^0 = \eta^* = 2$). With increasingly positive voltages $V = (kT/e_0)u$ the channel spends most of the time in the closed state B. Accordingly, the $I(V)$ curve exhibits rectifying behavior with a negative slope at larger voltages V. For large values of the equilibrium constant $\tilde{H}$ the channel starts to close already at voltages $V < 0$; the negative slope then becomes marginal.

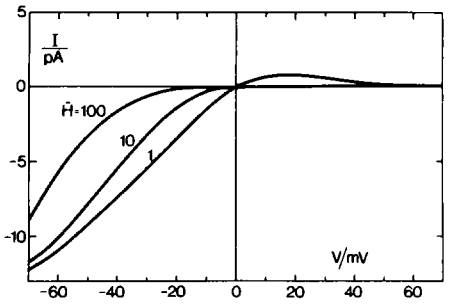

FIGURE 5 Current-voltage characteristic of a cationic channel ($z = 1$) that fluctuates between a conducting state A and a nonconducting state B. At high frequency of transitions A ⇌ B only an average current J is observed in the single-channel record. $J(V)$ has been calculated from Eqs. 14–21 for symmetrical aqueous solutions ($c' = c''$) under the condition $\tilde{H}^0 = \tilde{H}^* \equiv \tilde{H}$. ($\tilde{H}^0 = \tilde{k}^0_{AB}/\tilde{k}^0_{BA}$ and $\tilde{H}^* = \tilde{k}^*_{AB}/\tilde{k}^*_{BA}$ are the equilibrium constants for the transition A ⇌ B). The following parameter values have been used: $\nu'_A = \nu''_A = 2 \times 10^8\ s^{-1}$; $\mu'_A = \mu''_A = 10^8\ s^{-1}$; $\alpha'_e = \alpha''_e = 0.4$; $\alpha' = \alpha'' = 0.1$; $\eta^0 = \eta^* = 2$; $kT/e_0 = 25.7$ mV.

Reversal Potential and Ratios of Permeability and Unit Conductance

The reversal potential is the voltage at which the average current through the channel vanishes. In a biionic experiment with two permeable ionic species i and j, the reversal potential is given by the implicit equation $\Phi_i + \Phi_j = 0$. The experimental situation is particularly simple when ion species i is only present on the left and ion species j only on the right side and when i and j have identical concentrations ($c_i' = c_j'' = c$, $c_i'' = c_j' = 0$). Under this condition the reversal potential u_r of a channel with a single binding site and fixed conformation is given by the implicit relation

$$\frac{\tilde{\mu}_j' \exp(\alpha'' u_r/2) + \tilde{\mu}_j'' \exp(-\alpha' u_r/2)}{\tilde{\mu}_i' \exp(\alpha'' u_r/2) + \tilde{\mu}_i'' \exp(-\alpha' u_r/2)} \exp(u_r) = \frac{\tilde{\mu}_j' \tilde{\mu}_j''}{\tilde{\mu}_i' \tilde{\mu}_i''} \cdot \frac{K_j}{K_i}. \quad (22)$$

$K_i = \tilde{\rho}_i'/\tilde{\mu}_i'' = \tilde{\rho}_i''/\tilde{\mu}_i'$ and $K_j = \tilde{\rho}_j'/\tilde{\mu}_j'' = \tilde{\rho}_j''/\tilde{\mu}_j'$ are the equilibrium constants of ion binding at zero voltage (Läuger, 1973). When the voltage drop across the selectivity filter is small ($\alpha' \approx \alpha'' \approx 0$), Eq. 22 reduces to the Goldman equation

$$u_r = \ln\left(\frac{\tilde{\mu}_j' \tilde{\mu}_j''/\tilde{\mu}_j}{\tilde{\mu}_i' \tilde{\mu}_i''/\tilde{\mu}_i} \cdot \frac{K_j}{K_i}\right) \equiv \ln \frac{P_j}{P_i}. \quad (23)$$

The permeability ratio P_j/P_i, which is defined by Eq. 23, is introduced here merely as a convenient way to represent u_r. (Under the common assumptions that are used in the derivation of Goldman's equation (electrodiffusion under constant-field conditions) the quantity P_j/P_i is equal to the ratio P_j^*/P_i^* of the tracer permeability coefficients. For a channel with discrete binding sites P_j/P_i is, in general, different from P_j^*/P_i^*.)

A further quantity of interest is the ratio Λ_j/Λ_i of the single-channel conductances measured under symmetrical conditions ($c_i' = c_i'' = c$ or $c_j' = c_j'' = c$) in the limit $u \to 0$. For a channel with a single binding site and fixed conformation this ratio is given by (compare Eq. 13):

$$\frac{\Lambda_j}{\Lambda_i} = \frac{\tilde{\mu}_j' \tilde{\mu}_j''/\tilde{\mu}_j}{\tilde{\mu}_i' \tilde{\mu}_i''/\tilde{\mu}_i} \cdot \frac{K_j}{K_i} \cdot \frac{1 + cK_i}{1 + cK_j}. \quad (24)$$

Eqs. 23 and 24 mean, of course, that the permeability ratio is, in general, different from the conductance ratio:

$$s_{ij} \equiv \frac{P_j/P_i}{\Lambda_j/\Lambda_i} = \frac{1 + cK_j}{1 + cK_i} \neq 1. \quad (25)$$

Eq. 25, which holds for a channel with fixed conformation predicts that the permeability ratio P_j/P_i is larger than the conductance ratio Λ_j/Λ_i if ion species j is more strongly bound than ion species i ($K_j > K_i$). The difference between P_j/P_i and Λ_j/Λ_i becomes negligible at low ion concentrations (cK_i, $cK_j \ll 1$) i.e., far from saturation.

The analytical expressions for the reversal potential of a channel with two conducting states are rather cumbersome. It is easier to treat the problem numerically by calculating the probabilities $P(A^i)$, $P(B^i)$, etc., of the different occupancy states of Fig. 6 and introducing these values into Eq. 6. The reversal potential (and the permeability ratio P_j/P_i) is then obtained from the condition $\Phi_i + \Phi_j = 0$. In the calculation of $\Phi_i + \Phi_j$ the voltage dependence of the kinetic parameters has to be introduced explicitly, using Eqs. 16–21 together with the rate-theory expressions $k_{AB}^o = \tilde{k}_{AB}^o \exp(\eta^o u/2)$, $k_{BA}^o = \tilde{k}_{BA}^o \exp(-\eta^o u/2)$, $k_{AB}^* = \tilde{k}_{AB}^* \exp(\eta^* u/2)$, $k_{BA}^* = \tilde{k}_{BA}^* \exp(-\eta^* u/2)$ (compare Eq. 20).

In Fig. 7 values of $s_{ij} = (P_j/P_i)/(\Lambda_j/\Lambda_i)$ are plotted as a function of the rate constants $k_{AB}^o = k_{BA}^o$ of conformational transitions, assuming that the binding constant is identical for both ionic species in both conformational states ($K_A^i = K_A^j = K_B^i = K_B^j \equiv K$). For a channel with fixed conformation the ratio s_{ij} is equal to unity under this condition. In the case of a two-state channel, however, s_{ij} is a function of ionic concentration c even for $K_i = K_j$, as seen from Fig. 7. s_{ij} approaches the value k_{AB}^j/k_{AB}^i (= 100 in the example considered here) for $k_{AB}^o \to 0$ and becomes equal to unity for $k_{AB}^o \to \infty$. The results represented in Fig. 7 demonstrate that it is useful to measure P_j/P_i and Λ_j/Λ_i over a wide range of ionic concentrations in order to obtain information on the microscopic behavior of the channel.

CONCENTRATION DEPENDENCE OF MEAN LIFETIMES

A further prediction of the channel model depicted in Fig. 1 concerns the concentration dependence of mean lifetimes of channel states. We assume that the duration of conformational states A and B is long enough so that transitions can be directly observed in a single-channel current record. The probability that a channel that is in conformational state A makes a transition to state B within time dt may be

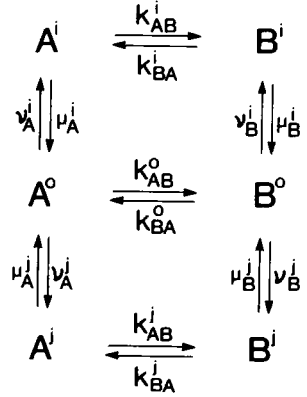

FIGURE 6 Channel with one binding site and two conformational states in the presence of permeable ion species i and j. A^o and B^o are empty states, A^i, A^j, B^i, and B^j are occupied states of the channel.

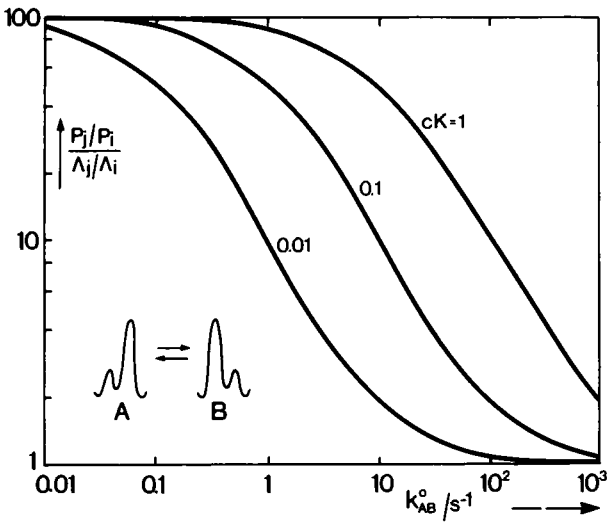

FIGURE 7 Permeability ratio P_j/P_i as obtained from the reversal potential $u_r \equiv \ln(P_j/P_i)$ in a biionic experiment with $c_i' = c_j'' = c$, $c_i'' = c_j' = 0$. Λ_j/Λ_i is the conductance ratio measured under symmetrical conditions at the same concentration ($c_i' = c_i'' = c$ or $c_j' = c_j'' = c$). $k^\circ_{AB} = k^\circ_{BA}$ are the rate constants of conformational transitions with empty binding site. $K \equiv K^i_A = K^j_A = K^i_B = K^j_B$ is the equilibrium constant of ion binding at zero voltage. The ratio $(P_j/P_i)/(\Lambda_j/\Lambda_i)$ is calculated for a channel with strongly asymmetric barriers and identical potential profiles for both ionic species, using $\tilde{\mu}'_A = \tilde{\mu}''_B = 10^{-7}\,s^{-1}$; $\tilde{\mu}''_A = \tilde{\mu}'_B = 10^{-7}\,s^{-1}$; $\tilde{k}^i_{AB} = \tilde{k}^i_{BA} = 10\,s^{-1}$; $\tilde{k}^j_{AB} = \tilde{k}^j_{BA} = 10^3\,s^{-1}$; $\alpha'_\epsilon = \beta''_\epsilon = 0$; $\alpha''_\epsilon = \beta'_\epsilon = 0.8$; $\alpha' = \alpha'' = \beta' = \beta'' = 0.1$; $\eta^\circ = 0$; $\eta^* = 0.8$; $z = 1$. This set of parameters is consistent with microscopic reversibility (Eq. 3) and corresponds to conformational states A and B, which are symmetric with respect to the barriers adjacent to the binding sites (see inset).

written as $dp = k_A dt$, the rate constant k_A being given by

$$k_A = \bar{P}(A^\circ)k^\circ_{AB} + \bar{P}(A^*)k^*_{AB}. \tag{26}$$

$\bar{P}(A^\circ) = 1 - \bar{P}(A^*)$ is the conditional probability that the channel is in state A°, given that it is in state A° or A^*. If the frequency of transitions A → B is much lower than the frequency of jumps of ions between binding site and aqueous solutions, the probabilities $\bar{P}(A^\circ)$ and $\bar{P}(A^*)$ are related by the steady state condition $\bar{P}(A^\circ)\nu_A = \bar{P}(A^*)\mu_A$ of a channel that is permanently in state A. This yields for the mean lifetime $\tau_A = 1/k_A$ of state A

$$\tau_A = \frac{\mu_A + \nu_A}{\mu_A k^\circ_{AB} + \nu_A k^*_{AB}}. \tag{27}$$

Thus, through the quantity $\nu_A = c'\rho'_A + c''\rho''_A$ (Eq. 1), the mean lifetime depends on the aqueous ion concentrations. Only when the transition frequencies are unaffected by the presence of the ion in the binding site ($k^\circ_{AB} = k^*_{AB}$) is the lifetime given by the usual concentration-independent relationship $\tau_A = 1/k^\circ_{AB}$. Evidence for a dependence of open-state lifetime on the nature and concentration of permeant ions has been obtained for acetylcholine-activated channels (Van Helden et al., 1977; Ascher et al., 1978; Marchais and Marty, 1979; Adams et al., 1981; Takeda et al., 1982), as well as for potassium channels (Swenson and Armstrong, 1981) and calcium channels (Nelson et al., 1984) in excitable membranes.

COUPLING OF FLUXES

If two permeable ion species i and j are present in the solutions bathing the membrane, two different fluxes Φ_i and Φ_j may be observed, for instance in a tracer flow experiment. For a permanently open channel with fixed potential profile, the fluxes of ion species i and j are given by (Läuger, 1973)

$$\Phi_i = \frac{\mu_j}{D} \cdot \nu''\mu''_i\,[\exp(zu - zu_i) - 1] \tag{28}$$

$$\Phi_j = \frac{\mu_i}{D} \cdot \nu''\mu''_j\,[\exp(zu - zu_j) - 1] \tag{29}$$

$$D \equiv \nu_i\mu_j + \nu_j\mu_i + \mu_i\mu_j \tag{30}$$

$$zu_i = \ln(c''_i/c'_i); \qquad zu_j = \ln(c''_j/c'_j). \tag{31}$$

From the form of Eqs. 28 and 29 it is clear that Φ_i and Φ_j do not obey the independence principle, since, for instance, Φ_i depends on c'_j and c''_j via $\nu_j = c'_j\rho'_j + c''_j\rho''_j$ in the denominator D. On the other hand, Φ_i vanishes when the system is in equilibrium with respect to ion species i ($u = u_i$), independent of the driving force for the other ion. This means that flux coupling does not occur in a one-site channel with fixed potential profile.

In a channel that fluctuates between two conformations A and B, the fluxes of different ion species may become coupled. A prerequisite for coupling is the condition that the frequency of conformational transitions is comparable to or larger than the frequency of ion jumps between binding site and aqueous phases. If state A has a low barrier to the left and a high barrier to the right, whereas state B has a high barrier to the left and a low barrier to the right, neither state is appreciably ion conducting. However, ions may pass through the channel by a cyclic process in which binding of an ion from the left side in state A is followed by a transition A → B and release of the ion to the right side (Fig. 8). Under these conditions the channel approaches the kinetic behavior of a carrier. When an ion has passed through the channel from left to right, the channel will be (with a high probability) in state B, in which binding of the next ion will take place preferentially from the right. Driving the cycle by a concentration difference $c'_j - c''_j > 0$ of ion species j thus induces a flux of a second ion species i in the opposite direction under the condition $c'_i = c''_i$. In other words, the channel exhibits negative flux coupling (or counter transport). It may be expected that coupling is particularly strong when the rates of conformational transitions in the empty state of the channel are low; this is the case when the rate constants of the transition $A^\circ \rightleftharpoons B^\circ$ are small, and/or when the ion concentrations are so high that the binding site is mostly occupied.

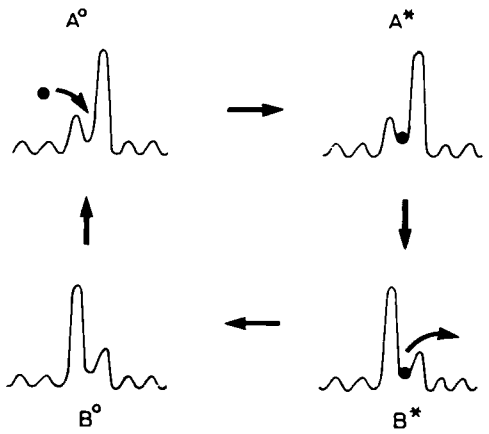

FIGURE 8 Carrier-like behavior of an ion channel resulting from transitions between state A with a high barrier to the right and state B with a high barrier to the left. During the cycle $A^\circ \rightarrow A^* \rightarrow B^* \rightarrow B^\circ$ an ion is translocated from left to right.

As an example we consider a hypothetical flux experiment in which ion species i and j are isotopes, so that all rate constants are the same for i and j. We also assume that states A and B are symmetrical with respect to the barriers of the selectivity filter (see inset of Fig. 9), with a ratio of 1:100 of the dissociation rate constants of the ion from the binding site. In Fig. 9 the coupling ratio Φ_i/Φ_j is given for a system that is in equilibrium with respect to ion species i ($c_i' = c_i''$, $u = 0$) and in which a flux $\Phi_j > 0$ is driven by a concentration difference $c_j' - c_j'' > 0$ of ion species j. Φ_i/Φ_j was calculated from Eq. 6 by solving the equations for the probabilities $P(A^i)$, $P(B^i)$, etc., numerically. It is seen from Fig. 9 that the flux Φ_j induces a countertransport of ion

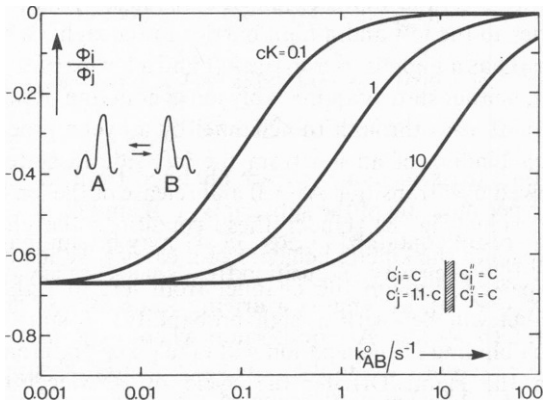

FIGURE 9 Coupling of fluxes Φ_i and Φ_j of two permeable (isotopic) ion species i and j. The system is in equilibrium with respect to ion species i ($c_i' = c_i''$, $u = 0$). $k^\circ_{AB} = k^\circ_{BA}$ are the rate constants of conformational transitions with empty binding site. $K \equiv K^i_A = K^j_A = K^i_B = K^j_B$ is the equilibrium constant of ion binding. The coupling ratio Φ_i/Φ_j is calculated for three different ion concentrations c with the following values of the kinetic parameters: $\mu^i_{A'} = \mu^j_{A'} = \mu^i_{B'} = \mu^j_{B'} = 0.1\ s^{-1}$; $\mu^i_{A''} = \mu^j_{A''} = \mu^i_{B''} = \mu^j_{B''} = 10\ s^{-1}$; $k^i_{AB} = k^j_{BA} = k^j_{AB} = k^i_{BA} = 1\ s^{-1}$. This set of parameters is consistent with microscopic reversibility (Eq. 3) and corresponds to conformational states A and B, which are symmetrical with respect to the barriers adjacent to the binding site (see inset).

species i ($\Phi_i < 0$). As expected, the absolute value of Φ_i/Φ_j is large for small values of the rate constants $k^\circ_{AB} = k^\circ_{BA}$ of conformational transitions with empty binding site. (For infinite height of the larger barrier, the ratio Φ_i/Φ_j approaches -1 in the limit $k^\circ_{AB}, k^\circ_{BA} \rightarrow 0$, corresponding to complete coupling). Furthermore, the coupling ratio increases with increasing ion concentration $c_i' = c_i'' = c_j' = c_j'' \equiv c$, i.e., with increasing occupancy of the binding site. At low ion concentrations and/or large values of $k^\circ_{AB} = k^\circ_{BA}$, coupling is lost ($\Phi_i/\Phi_j = 0$).

The isotope fluxes Φ_i and Φ_j are related to the unidirectional fluxes Φ' and Φ'' (Φ' is the flux from solution' to solution'', see Fig. 1):

$$\frac{\Phi'}{\Phi''} = \frac{c'}{c''} \cdot \frac{\Phi_i c_j'' - \Phi_j c_i''}{\Phi_i c_j' - \Phi_j c_i'} = \left(\frac{c'}{c''} \exp(zu)\right)^n. \qquad (32)$$

$c' = c_i' + c_j'$ and $c'' = c_i'' + c_j''$ are the total concentrations in solution' and solution'', respectively, and n is the so-called flux-ratio exponent. It is easily seen that under the conditions leading to countertransport (Fig. 9) n is always smaller than unity.

When the potential profile of both ion species in the channel is similar (or virtually identical as in the case of isotopes) flux coupling is always negative. On the other hand, if the two ion species interact very differently with the channel, situations are conceivable that lead to positive flux-coupling (cotransport). Positive flux-coupling occurs if the energy barriers for the two ion species are strongly different such that in state A ion i would enter more easily from the left and ion j more easily from the right, whereas in state B the binding site is accessible for i from the right and for j from the left. In this case passage of an ion i from left to right leaves the channel in state B, which then may return to state A by transfer of an ion j in the same direction. Thus, both cotransport and countertransport is possible in a channel with fluctuating potential profile. Coupling between fluxes of different ion species in this case does not require ion-ion interaction in the channel, but results from the correlation between successive transfer events.

NONEQUILIBRIUM DISTRIBUTION OF LONG-LIVED CHANNEL STATES

In the following we consider a channel that fluctuates between three conformational states A, B, and C (Hamill and Sakmann, 1981; Trautmann, 1982; Hamill et al., 1983); A may be the fully open state, C the closed state, and B a conductive substate. We assume that the lifetimes of these states are so long that the transitions can be directly observed in a single-channel current record (Fig. 10). A macroscopically observable transition, say, from A to B can result, at the microscopic level, from a transition $A^\circ \rightarrow B^\circ$ (binding site empty) or from a transition $A^* \rightarrow B^*$ (binding site occupied). (The distinction between these two elementary processes is always meaningful as long as

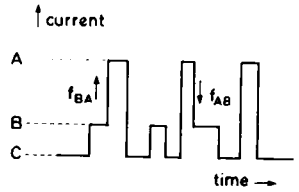

FIGURE 10 Single-channel record showing transitions among three different conformational states A, B, and C of the channel. f_{AB} and f_{BA} are the frequencies of transitions A → B and B → A, respectively.

the actual duration of a conformational transition is shorter than the mean lifetimes of the empty and occupied states of the binding site.) Accordingly, the microscopic description of the channel may be based on the scheme shown in Fig. 11.

From single-channel records such as those shown in Fig. 10 the frequency f_{XY} of transitions from state X to state Y may be obtained (X, Y = A, B, C). For a cyclic interconversion of three states:

the principle of microscopic reversibility requires that under equilibrium conditions the transition frequencies in both directions are the same ($f_{XY} = f_{YX}$). If, however, transitions between conformational states depend on the occupancy of ion binding sites, one may expect that the symmetry relationship $f_{XY} = f_{YX}$ no longer holds when ions are driven through the channel by an external force.

The expectation that f_{XY} and f_{YX} may become unequal in the presence of a driving force for ion flow is born out by an analysis of the reaction scheme of Fig. 11. Since A, B, and C are assumed to be observable conductance states, their lifetimes must be much larger than the average dwell time of ions in the binding sites. (If state C is nonconducting, the binding site may be assumed to be in fast exchange with one of the aqueous solutions.) The probabilities $P(X^\circ)$ and $P(X^*)$ for empty and occupied binding site are then given by the steady-state condition of a channel that is in a (quasi) permanent state X (X = A, B, C):

$$\frac{P(X^*)}{P(X^\circ)} = \frac{\nu_X}{\mu_X}. \tag{33}$$

Microscopic reversibility requires that the following relations hold (Läuger et al., 1980):

$$k^\circ_{AB}k^\circ_{BC}k^\circ_{CA} = k^\circ_{BA}k^\circ_{AC}k^\circ_{CB};$$

$$k^*_{AB}k^*_{BC}k^*_{CA} = k^*_{BA}k^*_{AC}k^*_{CB} \tag{34}$$

$$\frac{\nu'_X\mu'_X}{\nu''_X\mu''_X} = \frac{\nu''_X\mu'_Y}{\nu''_Y\mu''_X} \cdot \frac{k^*_{XY}k^\circ_{YX}}{k^\circ_{XY}k^*_{YX}} = \exp[z(u - u_o)]. \tag{35}$$

(X, Y = A, B, C). Since transitions X → Y may occur in the empty and in the occupied state of the binding site, the

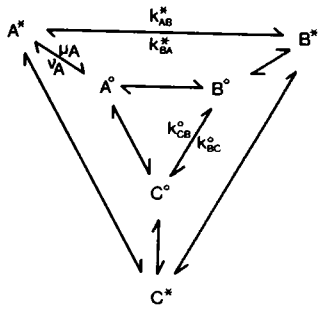

FIGURE 11 Transitions among three conformational states A, B, and C of a channel. States with empty binding site are denoted by A°, B°, and C°, states with occupied binding site by A*, B*, and C*.

total transition frequency f_{XY} is given by

$$f_{XY} = P(X^\circ)\,k^\circ_{XY} + P(X^*)\,k^*_{XY}. \tag{36}$$

The asymmetry in the transition frequencies may be expressed by the quantity χ_{XY}:

$$\chi_{XY} \equiv \frac{f_{XY} - f_{YX}}{f_{XY} + f_{YX}}. \tag{37}$$

χ_{XY} is obtained by calculating the probabilities $P(A^\circ)$, $P(A^*)$, etc., in the steady state (Appendix A). The result reads:

$$x_{AB} = \frac{1}{D_{AB}} \cdot [1 - \exp(zu - zu_o)]\,(q_{ABC} + q_{BCA} + q_{CAB}), \tag{38}$$

with the abbreviations:

$$q_{XYZ} \equiv (\nu'_X\nu''_Y - \nu''_X\nu'_Y) \cdot \left(\frac{\mu''_X}{\nu'_X}\nu_Z\,k^\circ_{XY}\,k^*_{YZ}\,k^*_{ZX} - \frac{\mu''_Y}{\nu'_Y}\mu_Z\,k^*_{XY}\,k^\circ_{YZ}\,k^\circ_{ZX}\right) \tag{39}$$

$$D_{AB} \equiv 2r_{AB}\,r_{BA}(r_{CA} + r_{CB}) + r_{AB}\,r_{BC}\,r_{CA} + r_{AC}\,r_{CB}\,r_{BA} \tag{40}$$

$$r_{XY} \equiv \mu_X\,k^\circ_{XY} + \nu_X\,k^*_{XY}. \tag{41}$$

The quantities χ_{BC} and χ_{CA} are obtained from Eq. 38 by cyclic permutation of the subscripts A, B, and C.

The result contained in Eqs. 38–41 may be summarized in the following way. Transition frequencies are asymmetric ($x_{XY} \neq 0$), as long as a driving force for ion flow is present ($u \neq u_o$). At equilibrium where $\exp(zu - zu_o)$ becomes equal to unity, the asymmetry disappears ($x_{XY} = 0$). This has to be expected, since the asymmetry of transition frequencies results from a nonequilibrium distribution of conformational states that is created by ion flow through the channel. Furthermore, by using Eq. 34 it may be shown that x_{XY} vanishes when the transition rate constants for empty and occupied binding site are identical ($k^\circ_{XY} = k^*_{XY}$). In general, however, k°_{XY} and k^*_{XY} are different, since the presence of a charge in the binding site changes the energy of the different conformational states.

Another limiting case in which the transition frequen-

cies become symmetrical is given by the condition (Ascher et al., 1978; Marchais and Marty, 1979) that conformational transitions can occur only when the binding site is empty ($k^*_{XY} = 0$).

The problem of cyclic interconversion of channel states discussed here has a well-known counterpart in ordinary chemical kinetics (Skrabal, 1930; Hearon, 1953). In a cyclic reaction among three chemical species A, B, and C an equilibrium state may be maintained, in principle, by a fast clockwise reaction A → B → C → A and a simultaneous slow counter-clockwise reaction A → C → B → A. This possibility is excluded by the principle of microscopic reversibility or detailed balance (Onsager, 1931), which requires that in the equilibrium state the rates of each elementary reaction step X → Y are the same in both directions. If, however, a nonequilibrium steady state is maintained by continuous supply or withdrawal of reactants, the reaction rates become unequal in the forward and in the backward direction. In the case of the ionic channel, the transition frequencies become asymmetric when interconversion among the conformational states is coupled to a dissipative process, the transfer of ions from high to low electrochemical potential. In the presence of a difference of electrochemical potential the cycle is driven preferentially in one (clockwise or counterclockwise) direction, meaning that $f_{AB} - f_{BA} = f_{BC} - f_{CB} = f_{CA} - f_{AC} \neq 0$.

A simple situation leading to a pronounced asymmetry is given by the following example. Assume that in the transitions A → B and B → C the binding site moves within the membrane dielectric towards the right. If the permeable ion is positively charged and if the left-hand aqueous phase has a high positive potential, the rates of the transitions A* → B* and B* → C* (binding site occupied) are strongly enhanced. The back transition C → A may proceed via the (weakly voltage-dependent) pathway C° → A°. The cycle A* → B* → C* → C° → A° → A* (during which a cation is transferred from left to right) is then driven by the electric field so that the overall cycle A → B → C → A becomes predominant over the inverse cycle A → C → B → A. This may be shown in a more explicit way, assuming the following set of parameters: $\tilde{k}^\circ_{AB} = \tilde{k}^\circ_{BA} = \tilde{k}^\circ_{BC} = \tilde{k}^\circ_{CB} = \tilde{k}^*_{AC} = \tilde{k}^*_{CA} \equiv p$, $\tilde{k}^*_{AB} = \tilde{k}^*_{BA} = \tilde{k}^*_{BC} = \tilde{k}^*_{CB} = \tilde{k}^\circ_{AC} = \tilde{k}^\circ_{CA} \equiv q \gg p$, $\tilde{\mu}'_A = \tilde{\mu}'_B = \tilde{\mu}'_C = \tilde{\nu}''_A = \tilde{\nu}''_B = \tilde{\nu}''_C \equiv r$, $\tilde{\mu}''_A = \tilde{\mu}''_B = \tilde{\mu}''_C = \tilde{\nu}'_A = \tilde{\nu}'_B = \tilde{\nu}'_C \equiv s \gg r$, $u_o = 0$. Eq. 38 then reduces to

$$x_{AB} = \frac{1 - \exp(-zu)}{1 + \exp(-zu) + 2\dfrac{k^*_{BA}}{k^*_{BC}}\left(1 + \dfrac{\nu''_C}{\mu'_C}\dfrac{k^*_{CB}}{k^\circ_{CA}}\right)}. \tag{42}$$

It may be further assumed that k°_{CA}, ν''_C, and μ'_C are virtually voltage-independent and that the voltage-dependence of k^*_{BA}, k^*_{BC}, and k^*_{CB} is given by $k^*_{BA} = k^*_{CB} = q \cdot \exp(-zu/4)$ and $k^*_{BC} = q \cdot \exp(zu/4)$, corresponding to translocations of the binding site over half of the membrane dielectric in the transitions A → B and B → C. This gives (with $\exp(-zu/4) \equiv \lambda$):

$$x_{AB} = \frac{1 - \lambda^4}{1 + 2\lambda^2(1 + \lambda) + \lambda^4}. \tag{43}$$

Thus, for $u \gg 1$ ($\lambda \approx 0$), x_{AB} approaches unity, meaning that the cycle is driven exclusively in one direction at large voltage.

CONCLUSION

The existence of multiple conductance states of ionic channels is suggested by current concepts of protein dynamics and is directly supported by single-channel experiments. Lifetimes of individual conformational states may be far below the theoretical limit of time resolution of single-channel experiments. The existence of such hidden substates may strongly influence the observable (time-averaged) properties of a channel. A channel exhibiting fast, voltage-dependent fluctuations between different conductance states may behave as an intrinsic rectifier. In a biionic experiment the reversal potential exhibits an unusual concentration dependence that is different from the behavior of a channel with fixed conformation. Furthermore, in the presence of more than one permeable ion species, coupling between ionic fluxes may occur, even when the channel has only a single ion-binding site. In special situations the rate of ion translocation becomes limited by the rate of conformational transitions, meaning that the channel approaches the kinetic behavior of a carrier.

Of particular interest is the possibility that the rate constants of transitions between conformational states depend on the occupancy of ion-binding sites in the transport pathway. In this case the lifetimes of conductance states are influenced by the nature and the concentration of permeable ions, a phenomenon that has been observed with several types of ionic channels.

If the transition probabilities are different for empty and occupied states of the binding site, a nonequilibrium distribution of conformational states is created when ions are driven through the channel by an external force. A channel that fluctuates between three observable (long-lived) conductance states A, B, and C may then exhibit an asymmetry in the transition frequencies ($f_{XY} \neq f_{YX}$). This apparent violation of microscopic reversibility results from coupling between conformational transitions and ion flow.

I thank Dr. E. Frehland and Dr. H.-A. Kolb for interesting discussions, and Dr. H.-J. Apell for help in the computational work.

This work has been supported by the Deutsche Forschungsgemeinschaft (Sonderforschungsbereich 156).

Received 17 February 1984 and in final form 7 August 1984.

APPENDIX A

Derivation of Eq. 38

To calculate the transition frequency f_{XY}, we introduce the conditional probability $\bar{P}(X^*)$ that the channel is in state X^* (given that it is in state X^* or X°). $\bar{P}(X^*)$ is connected with the probability $P(X^*)$ of state X^* and with the total probability P_X of state X (X° or X^*) by the relation $P(X^*) = P_X\bar{P}(X^*)$. According to Eq. 33 the conditional probabilities $\bar{P}(X^*)$ and $\bar{P}(X^\circ) = 1 - \bar{P}(X^*)$ are given by

$$\bar{P}(X^*) = \frac{\nu_X}{\nu_X + \mu_X}; \qquad \bar{P}(X^\circ) = \frac{\mu_X}{\nu_X + \mu_X}. \tag{A1}$$

Using Eqs. A1 the transition frequency $f_{XY} = P(X^*)\,k^*_{XY} + P(X^\circ)\,k^\circ_{XY}$ is obtained as

$$f_{XY} = \frac{P_X}{\nu_X + \mu_X}(\nu_X k^*_{XY} + \mu_X k^\circ_{XY}) \equiv P_X s_{XY}. \tag{A2}$$

The probabilities P_X, P_Y, and $P_Z = 1 - P_X - P_Y$ may be calculated from the steady-state conditions $dP_X/dt = 0$, $dP_Y/dt = 0$

$$\frac{dP_X}{dt} = -(s_{XY} + s_{XZ})P_X + s_{YX}P_Y + s_{ZX}P_Z = 0 \tag{A3}$$

$$\frac{dP_Y}{dt} = -(s_{YX} + s_{YZ})P_Y + s_{XY}P_X + s_{ZY}P_Z = 0. \tag{A4}$$

The result reads

$$P_X = (s_{YX}s_{ZX} + s_{ZY}s_{YX} + s_{YZ}s_{ZX})/Q \equiv Q_X/Q \tag{A5}$$

$$P_Y = (s_{XY}s_{ZY} + s_{ZX}s_{XY} + s_{XZ}s_{ZY})/Q \equiv Q_Y/Q \tag{A6}$$

$$P_Z = (s_{XZ}s_{YZ} + s_{XY}s_{YZ} + s_{YX}s_{XZ})/Q \equiv Q_Y/Q \tag{A7}$$

$$Q \equiv Q_X + Q_Y + Q_Z. \tag{A8}$$

The quantity χ_{AB} (Eq. 38) is then obtained (after a lengthy calculation) by combination of Eqs. 1, 2, 34, 35, 37, A2, A5, and A6.

REFERENCES

Adams, D. J., W. Nonner, T. M. Dwyer, and B. Hille. 1981. Block of endplate channels by permeant cations in frog skeletal muscle. *J. Gen. Physiol.* 78:593–615.

Ascher, P., A. Marty, and T. O. Neild. 1978. Lifetime and elementary conductance of the channels mediating the excitatory effects of acetylcholine in *Aplysia* neurons. *J. Physiol. (Lond.).* 278:177–206.

Auerbach, A., and F. Sachs. 1983. Flickering of a nicotinic ion channel to a subconductance state. *Biophys. J.* 42:1–10.

Frauenfelder, H., G. A. Petsko, and D. Tsernoglu. 1979. Temperature-dependent X-ray diffraction as a probe of protein structural dynamics. *Nature (Lond.).* 280:558–563.

Frehland, E. 1979. Theory of transport noise in membrane channels with open-closed kinetics. *Biophys. Struct. Mechanism.* 5:91–106.

Gunning, R. 1983. Kinetics of inward rectifier gating in the eggs of the marine polychaete, *Neanthes arenaceodentata*. *J. Physiol. (Lond.).* 342:437–451.

Hamill, O. P., J. Bormann, and B. Sakmann. 1983. Activation of multiple-conductance state chloride channels in spinal neurons by glycine and GABA. *Nature (Lond.).* 305:805–808.

Hamill, O. P., and B. Sakmann. 1981. Multiple conductance states of single acetylcholine receptor channels in embryonic muscle cells. *Nature (Lond.).* 294:462–464.

Hearon, J. Z. 1953. The kinetics of linear systems with special reference to periodic reactions. *Bull. Math. Biophys.* 15:121–141.

Hille, B. 1971. The permeability of the sodium channel to organic cations in myelinated nerve. *J. Gen. Physiol.* 58:599–619.

Hille, B., and W. Schwarz. 1978. Potassium channels as multi-ion single-file pores. *J. Gen. Physiol.* 72:409–442.

Huber, R., J. Deisenhofer, P. M. Colman, M. Matshushima, and W. Palm. 1976. Crystallographic structure studies of an IgG molecule and an Fe fragment. *Nature (Lond.).* 264:415–420.

Karplus, M., and J. A. McCammon. 1983. Dynamics of proteins: Elements and function. *Annu. Rev. Biochem.* 52:263–300.

Lakowicz, J. R., B. P. Maliwal, H. Cherek, and A. Balter. 1983. Rotational freedom of tryptophan residues in proteins and peptides. *Biochemistry.* 22:1741–1752.

Läuger, P. 1973. Ion transport through pores: a rate-theory analysis. *Biochim. Biophys. Acta.* 311:423–441.

Läuger, P., W. Stephan, and E. Frehland. 1980. Fluctuations of barrier structure in ionic channels. *Biochim. Biophys. Acta.* 602:167–180.

Marchais, D., and A. Marty. 1979. Interaction of permeant ions with channels activated by acetylcholine in *Aplysia* neurons. *J. Physiol. (Lond.).* 297:9–45.

Nelson, M. T., R. I. French, and B. K. Krueger. 1984. Single calcium channels from rat brain in planar bilayer membranes. *Nature (Lond.).* 308:77–80.

Onsager, L. 1931. Reciprocal relations in irreversible processes. I. *Phys. Rev.* 37:405–426.

Parak, F., E. N. Frolov, R. L. Mössbauer, and V. I. Goldanskii. 1981. Dynamics of metmyoglobin crystals investigated by nuclear gamma resonance absorption. *J. Mol. Biol.* 145:825–833.

Parlin, R. B., and H. Eyring. 1954. Membrane permeability and electrical potential. *In* Ion Transport Across Membranes. H. T. Clarce, editor. Academic Press Inc., New York. 103–118.

Sakmann, B., and E. Neher. editors. 1983. Single-Channel Recording. Plenum Publishing Corp., New York. 1–503.

Sakmann, B., A. Noma, and W. Trautwein. 1983. Acetylcholine activation of single muscarinic K^+ channels in isolated pacemaker cells of the mammalian heart. *Nature (Lond.).* 303:250–253.

Sakmann, B., and G. Trube. 1984. Conductance properties of single inwardly rectifying potassium channels in ventricular cells from guinea pig heart. *J. Physiol. (Lond.).* 347:641–657.

Sandblom, J., G. Eisenman, and J. Hägglund. 1983. Multioccupancy models for single filing ionic channels: theoretical behaviour of a four-site channel with three barriers separating the sites. *J. Membr. Biol.* 71:61–78.

Skrabal, A. 1930. Zur Theorie der periodischen Reaktionen im homogenen System. *Z. Phys. Chem. Abt. B.* 6:382–422.

Swenson, R. P. Jr., and C. M. Armstrong. 1981. K^+ channels close more slowly in the presence of external K^+ and Rb^+. *Nature (Lond.)* 291:427–429.

Takeda, K., P. H. Barry, and P. W. Gage. 1982. Effects of extracellular sodium concentration on null potential, conductance and open time of endplate channels. *Proc. R. Soc. Lond. B. Biol. Sci.* 216:225–251.

Trautmann, A. 1982. Curare can open and block ionic channels associated with cholinergic receptors. *Nature (Lond.).* 298:272–275.

Urban, B. W., S. B. Hladky, and D. A. Haydon. 1980. Ion movement in gramicidin pores. An example of single-file transport. *Biochim. Biophys. Acta.* 602:331–254.

Van Helden, D., O. P. Hamill, and P. W. Gage. 1977. Permeant ions alter endplate channel characteristics. *Nature (Lond.).* 269:711–713.

Wagner, G. 1983. Characterization of the distribution of internal motions in the basic pancreatic trypsin inhibitor using a large number of internal NMR probes. *Quart. Rev. Biophys.* 16:1–57.